ISSN 2229-5518

Finite element analysis of electromagnetic bulging of sheet metals

Ali M. Abdelhafeez, M. M. Nemat-Alla, M. G. El-Sebaie

Abstract— Electromagnetic forming is a high velocity forming technique that uses high pulsed current to produce repulsion electromagnetic pressure between a forming coil and the workpiece. In the FE modelling of such process two physical models are involved; electromagnetic model and mechanical model in addition to a method of coupling these models. Two well-known coupling schemes were previously used; strong coupling and loose coupling which are either takes long simulation time or gives inaccurate results. Therefore some modifications were made to the loose coupling scheme to give accurate simulation results in small duration.

Material strain hardening models which describe mechanical behaviour of the used material at such high speed forming process are of primary importance to get accurate simulation results. Two hardening models were used in previous researches on this process. But no comparison between them was made to conclude the most accurate model in describing hardening behaviour of the used material.

The current investigations introduce a comparison between two hardening material models that used in previous researches. The comparison was made between results of numerical simulations and experimental results obtained from literature. The used FE model is based on modified loose coupling scheme. Simulation results reveal that rate dependant power law hardening model gives the most accurate results with small average deviation compared with experimental data. It reveals also that modified loose coupling between mechanical and electromagnetic aspects is an efficient tool for getting accurate simulation results within short time.

Index Terms— High speed forming, Electromagnetic forming, bulging of sheet metals, FEM, Strain hardening models, modified loose coupling method.

1 INTRODUCTION

ELECTROMAGNETIC forming (EM Forming) process depends on generating high intensity transient magnetic fields by forcing high current to flow through a coil positioned very close to the workpiece. When a pulsed high current flows through the coil, a transient magnetic field is produced around the coil. This changing field induces eddy currents in the workpiece opposed in direction with the coil current. The eddy currents of the workpiece produce a magnetic field. The magnetic fields of the coil and the workpiece repel each other, producing high repulsive pressure. This pressure is considered as the driving force of deformation. The pulsed high current can be generated by charging capacitor banks at high voltage and suddenly drain all the charge in the coil.

Because EM forming characterizes by high deformation velocity and no-contact between tool and workpiece, the forming limits of metal sheets can be enhanced [1] in addition to reducing springback and wrinkling [2]. These characteristics drive the researchers to try to benefit from it; especially in the manufacturing of light weight vehicles body which is fabricated from Aluminium alloys. Because of Aluminium low fracture strain and high springback; EMF is the ideal forming technique to be used for overcoming these drawbacks and benefiting from its high electrical conductivity.

- *Ali M. Abdelhafeez is currently pursuing master degree program in metal forming at Assiut University, Egypt, PH-+201007735899. E-mail: a.m.abdelhafeez@gmail.com*
- *M. M. Nemat-Alla, professor of materials science, Assiut University, Egypt.*
- *M. G. El-Sebaie, professor of metal forming, Assiut University, Egypt.*

Several investigations had been done on EM forming in which few were related to electromagnetic sheet metals bulging. One of such early investigations was made by Takatsu et al. [3] in which finite difference modelling and experimental verification was made. Takatsu experimental work considered today as a benchmark in EM bulging of sheet metals. His experimental data had been used by many other previous researchers to verify their numerical simulation.

On computing technology advancement, numerical methods began to take increasing role in modelling and simulation of metal forming processes. Fenton and Daehn [4] used a 2D finite difference code to simulate EM forming process with a fully electromagnetic–mechanical coupling. In order to validate their computer code the results of the experimental work of Takatsu et al. [3] were used as benchmarks. Steinberg work hardening material model was adopted. Although their material model ignores strain rate effects, the results showed good agreement with experimental results. This may be attributed to the use of material model that has much higher initial yield stress (93 MPa) than the actual value (22 MPa [5]).

El-Azab et al. [6] reported the future needs in modelling EM forming as two major challenges; numerical challenges and material modelling challenges. They claimed that numerical solution of the general fully coupled problem has not been previously achieved. On the other hands the material challenges are appear in adopting strain rate and temperature dependency through the deformation processes. Only their net effects on the deformation process can be observed in laboratory tests while experimental observation of their effect with time and deformation is difficult due to the high speed of deformation and biaxiallity of strains.

Correia et al. [7] made a trial to overcome modelling challenges of EM forming. They used rate dependant power law for describing strain hardening behaviour of Takatsu et al. [3] disk material. They considered a simple model of EM bulging process, in which the mechanical and electromagnetic aspects were treated as two independent problems. ABAQUS/Explicit FEM software was used to simulate the deformation of the sheet as explained in Takatsu et al. [3]. The magnetic spatial and temporal pressure distributions were determined using finite difference code which was implemented in ABAQUS user subroutine named VDLOAD to solve magnetic diffusion equations. The obtained pressure was then used as a load to the mechanical problem to calculate the deformation. This coupling technique is known by loose coupling. Although they used strain rate dependent power law, their results are not in good agreement with previous experimental results of Takatsu et al. [3]. This may be due to the consideration of loose coupling scheme without modifications that gives more accurate simulation results as mentioned by Hashimoto et al. [8].

Siddiqui et al. [9] enhanced electromagnetic part of Correia model [7] for getting more accurate simulation results. They compared the obtained simulation results with experimental data [3] and a good agreement was noticed. They concluded that mesh size effects have negligible influence on results due to small thickness size of workpiece.

Recently, Cui et al. [10] simulated experimental work of Takatsu et al. [3] using ANSYS multi-physics FEM software. Strong coupling scheme was used which accounts for magnetic pressure change with workpiece deformation. Following Fenton and Daehn [4], the simplified Steinberg Material hardening model was used. The simulation results were in good agreement with experimental results but simulation process was time consuming.

Finally from the previous literature survey it can be concluded that two material hardening models were used to describe Takatsu [3] disk material behaviour. These two material hardening models are Steinberg model, and rate dependant power law model. Previous researchers used different FE simulation models that utilized these hardening models and good agreement was obtained. But right comparison between these hardening models must be with the same FE model to conclude the most accurate one.

In this research, an FE model was established based on modified loose coupling between electromagnetic and mechanical aspects. This loose coupling strategy was considered before by many other researchers [7], [11], [12], [13]. The model was used to compare these hardening models to determine the most accurate one in describing mechanical behaviour of the used material at these conditions.

2 PROCESS MODELLING

2.1 Electrical system model

EM sheet metals bulging is a high velocity forming technique in which there is a spiral flat coil positioned near to a flat circular blank workpiece. A high repulsion pressure produced between coil and workpiece when transient high electrical current passes in the coil. Typical process setup is shown in Fig. (1) and dimensions are given in table (1). This setup could be modelled electrically by two mutually coupled circuits that shown in Fig. (2).

TABLE (1)

COIL AND WORKPIECE DIMENSIONS.

Coil		Workpiece	
Major radius	32 mm	Thickness	0.5 mm.
No. of turns	5	Bulged diameter	80 mm.
pitch	5.5 mm	Overall diameter	110 mm.
Coil/ Workpiece separation distance = 1.6 mm			

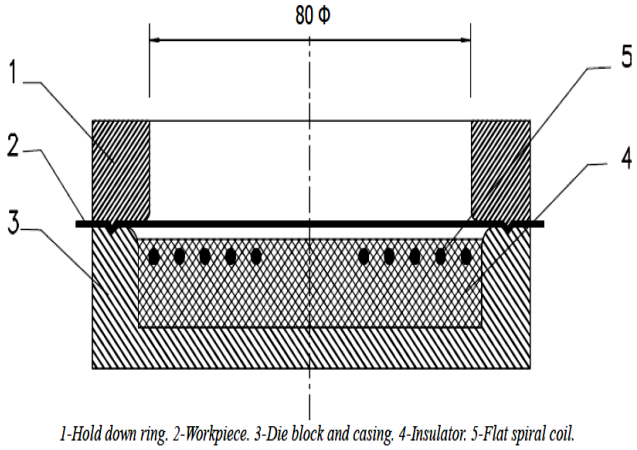

Fig. 1. Typical setup of EM bulging of sheet metals.

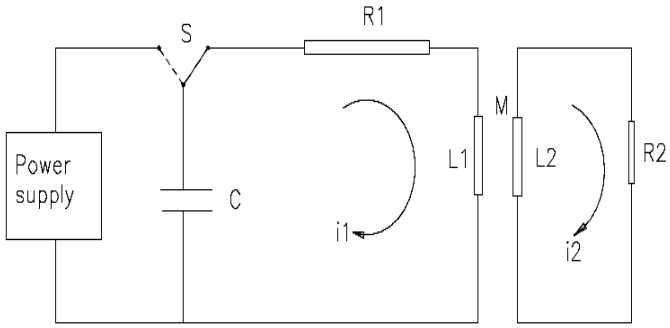

Fig. 2. Electrical model of the process.

Governing differential equations of these magnetically coupled circuits according to Takatsu et al. [3], is:

$$\left.\begin{aligned} L_1\frac{d}{dt}i_1(t)+\frac{d}{dt}(M.i_2(t))+R_1.i_1(t)+\frac{1}{c}\int_0^t i_1(t)dt=0; \\ \frac{d}{dt}(L_2.i_2(t))+\frac{d}{dt}(M.i_1(t))+R_2.i_2(t)=0 \end{aligned}\right\} \quad (1)$$

With initial conditions:

$$i_1(0)=0,\ i_2(0)=0,\ [L_1\frac{d}{dt}i_1]_{t=0}=V_0$$

Where, L_1, L_2 are inductance of the coil and workpiece circuit; M is mutual inductance between the two circuits; R_1, R_2 are electrical resistances of the coil and workpiece circuit; c capacitance of discharge circuit; V_0 is initial discharge voltage of the capacitor banks; $i_1(t)$ is discharging current as function of time for the coil circuit; $i_2(t)$ is induced current function of time for the workpiece circuit.

These two simultaneous equations have the mutual inductance term M which represent the magnetic coupling between the two circuits. The mutual inductance M and the self-inductance of the workpiece L_2 change with the workpiece deformation and deformation depends mainly on M and L_2. This interdependency makes the mathematical solution of these two equations almost difficult unless using numerical methods with simplifying assumptions. Assuming that M and L_2 are constants and not depend on deformation will simplify this problem. This assumption is part of loose coupling technique used in tying electromagnetic and mechanical aspects. The equivalent circuit model now could be obtained, and the reduced equation for the current will be [8]:

$$L_c \frac{d}{dt} i_c(t) + R_c \cdot i_c(t) + \frac{1}{c_c} \int_0^t i_c(t) dt = V_0 \quad (2)$$

With initial conditions:

$$i_c(0) = 0, [L_c \frac{d}{dt} i_c]_{t=0} = V_0$$

Where, L_c is total inductance of the system; R_c is total electrical resistance of the system; C_c is total capacitance of the system; $i_c(t)$ is the current passing in the coil; V_0 is initial discharge voltage of the capacitor banks.

The solution of Eq. (2) is given by [14]:

$$i(t) = \frac{V_0}{\omega L_c} e^{-\beta t} \sin(\omega t) \quad (3)$$

Where,

$$\omega = \sqrt{\frac{1}{L_c C_c} - (\frac{R_c}{2L_c})^2}$$

Values of these electrical parameters are given by table (2).

TABLE (2)

PROCESS ELECTRICAL PARAMETERS.

Total inductance L_c	2.86	µH
Total Capacitance C_c	40	µF
Charging voltage V_0	6	kV
Total Resistance R_c	28.5	mΩ

It can be noticed that the electric current function has an exponentially decayed sinusoidal wave form as shown in Fig. (3).

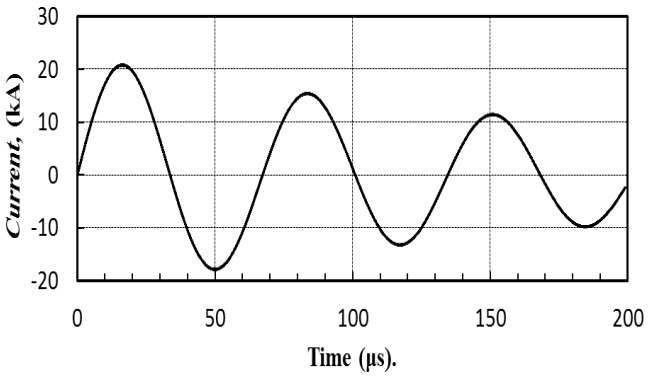

Fig. 3. Variation of electric current i(t) with time.

2.2. Magnetic pressure model

Magnetic pressure generated from magnetic field of the coil current is the driving force of workpiece deformation. Its distribution over the workpiece is not uniform and it is varying with time and with workpiece deformation. Thus magnetic pressure is dependent on workpiece deformation and deformation is dependent on applied magnetic pressure. This interdependency makes perfect determination of this pressure depends mainly on the electromagnetic-mechanical aspects coupling scheme used.

Assuming magnetic pressure to be independent on workpiece deformation will simplify the analysis with small relative errors in results. Therefore the general magnetic pressure function $P(r,t)$ can be considered as a function of blank radius multiplied by a pressure function of time, i.e.

$$P(r,t) = f(r) \cdot p(t) \quad (4)$$

The temporal variation of magnetic pressure was expressed before [8] as:

$$p(t) = \frac{B(t)^2 - B_{diff}(t)^2}{2\mu_0} \quad (5)$$

Where, $B(t)$ is magnetic flux density between workpiece and coil; $B_{diff}(t)$ is diffused flux density; and μ_0 is magnetic permeability of the air.

Magnetic flux density; $B(t)$; is given by [15],

$$B(t) = K \mu_0 i(t) \quad (6)$$

Where; K is constant depends on workpiece and coil geometry and skin depth.

The diffused magnetic flux can be neglected for non-magnetic materials like Aluminium [16], thus;

$$p(t) = \frac{B(t)^2}{2\mu_0} \quad (7)$$

Consequently from (3), (6) and (7) the final form of temporal pressure behaviour is

$$p(t) = \frac{1}{2} \mu_0 K^2 (\frac{V_0}{\omega L_c})^2 e^{-2\beta t} \sin^2(\omega t) \quad (8)$$

Such variation of temporal behaviour of the magnetic pressure is shown in Fig. (4).

The spatial distribution at a given time can be determined by studying the magnetic flux density distribution over the disk radius. This distribution can be found by numerically solving Maxwell equations of electromagnetism for specific coil-workpiece geometry. Such numerical solution is beyond the scope of this research paper.

Previous calculated data [3] of spatial pressure distribution at time of maximum pressure value was used; after normalizing; to determine spatial distribution function. Normalized data was obtained by dividing all pressure values with maximum *p(t)* value and is shown in fig. (5).

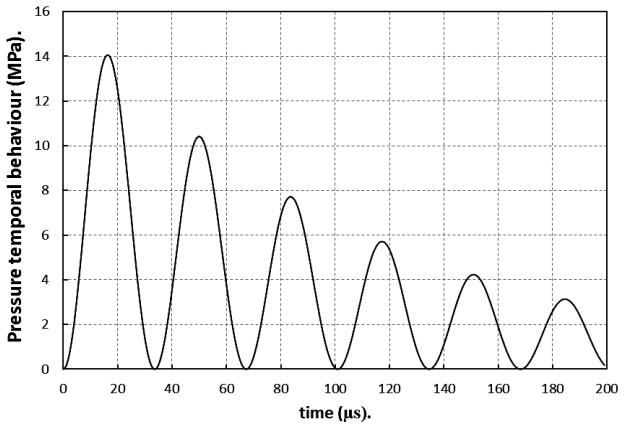

Fig. 4. Temporal behaviour of magnetic pressure.

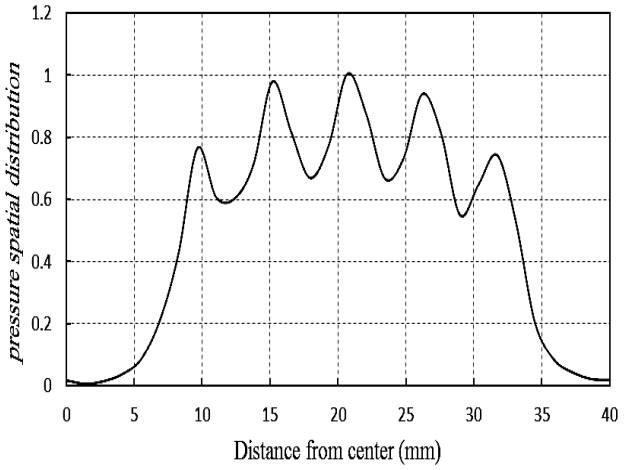

Fig. 5. Pressure spatial distribution over workpiece radius.

Now magnetic pressure function has been identified and determined. This function is entered to the mechanical FE model as surface pressure on the bottom surface of the blank with spatial and temporal variation specified before.

2.3 Mechanical FE model

The magnetic pressure calculated by (4) is used as boundary condition to the structure model and entered to an FEM simulation package, an implicit dynamic finite element code, which is used in sheet deformation analysis. The dynamic equilibrium equation is given by (9), and the Newmark time integration method is used to solve it [17].

$$M\ddot{u} + C\dot{u} + Ku = F \tag{9}$$

Where *M* represents the mass matrix (Kg), *C* is the damping matrix (Kg/s), *K* is the stiffness matrix (Kg/s²), *F* is load vector (N). According to Takatsu experimental work [3], workpiece mechanical and electrical properties are listed in table (3).

TABLE (3)

WORKPIECE MATERIAL PROPERTIES

Density	2750 Kg/m^3
Young's Modulus	80.7 GPa
Poisson's ratio	0.33
Yield stress	22 MPa.
Electric conductivity	34.45 MS/m

The workpiece is meshed with quadrilateral finite-membrane-strain element with reduced integration points on its surface and 9 integration points through its thickness. Total number of elements is 4000 and the meshed workpiece is shown in fig. (6).

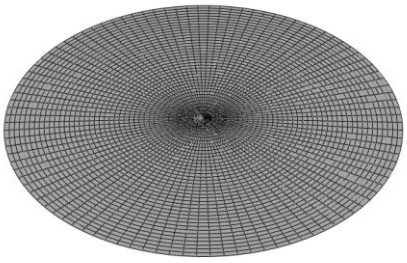

Fig. 6.Non-deformed workpiece mesh.

During deformation, workpiece outer perimeter is considered to be fixed.

There are two hardening models that are extensively used in modelling JIS A1050-O material which used in Takatsu et al. [3] experimental work. Simplified Steinberg model [4], [10] as given by (10), and rate dependent power law [7], [9] as given by (11).

$$\bar{\sigma} = 93(1+125\bar{\varepsilon})^{0.1} \tag{10}$$

$$\bar{\sigma} = 201\,\bar{\varepsilon}^{\,0.27}\,\dot{\bar{\varepsilon}}^{\,0.075} \tag{11}$$

Where $\bar{\sigma}$ is the effective stress in MPa; $\bar{\varepsilon}$ is the effective strain. These hardening models are shown in fig. (7).

To decide the most accurate model in describing hardening behaviour of this material; An FE simulation was built which is based on a modified loose coupling scheme. Next section describes this coupling scheme.

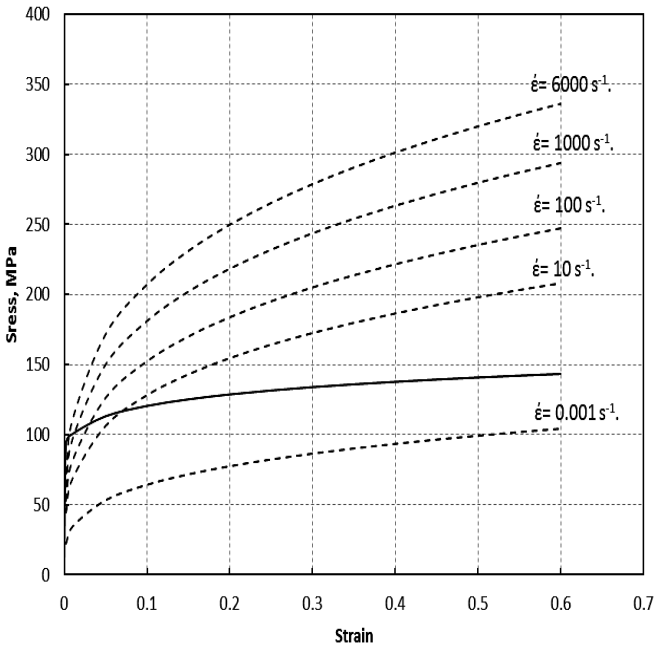

Fig. 7. Effective stress-strain diagrams for used hardening models (dashed lines represent rate dependent model and solid line represents Steinberg model).

2.4 Modified loose coupling scheme

Loose coupling depends on finding the magnetic pressure spatial and temporal distribution independent of workpiece deformation. This is of course untrue and always gives overestimated simulation results. A modification of this coupling scheme to get more accurate results is mentioned by Hashimoto et al. [8]. They reported that only the first wave of current affects deformation of workpiece.

Thus the modified loose coupling scheme considers only the first wave of current to determine magnetic pressure temporal behaviour. On the other hand, the spatial pressure distribution function $f(r)$ was specified before from electromagnetic FE simulation. Therefore the total load to be applied on the workpiece surface is $P(r,t) = p(t)|_{modified} \cdot f(r)$, where $f(r)$ is as given by Fig. (5), and $p(t)|_{modified}$ is given by (12) and shown in fig. (8).

$$p(t)|_{modified} = \begin{cases} \frac{1}{2}\mu_0 K^2 i(t)^2, & t \le \tau \\ 0, & t > \tau \end{cases} \qquad (12)$$

Where, τ is the periodic time of current wave $i(t)$ and equals 67 μs.

3 FE SIMULATION AND RESULTS ANALYSIS

Two runs of the simulation were done each with one of the hardening models previously listed.

The final deformed profile of the workpiece for each hardening model is presented in fig. (9) in conjunction with, Takatsu [3] experimental data. It is clear that the used strain hardening models have a great effect on the simulation results. Obviously, there is a moderate agreement between the experimental results and the rate dependent hardening model simulation results. In addition to a large deviation between the other hardening model simulation results and Takatsu results are clearly appeared.

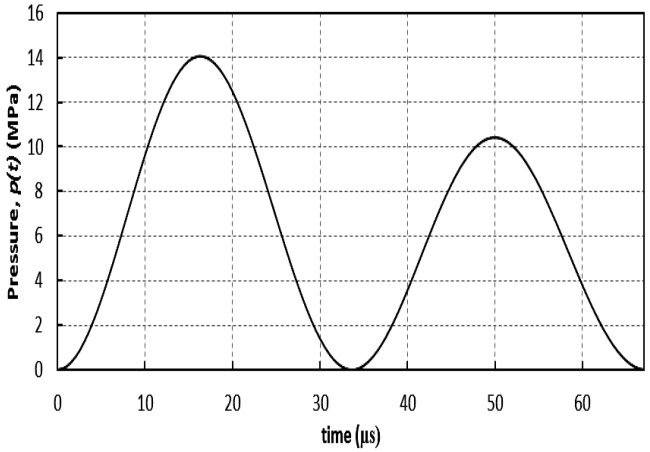

Fig. 8. Modified pressure temporal behaviour.

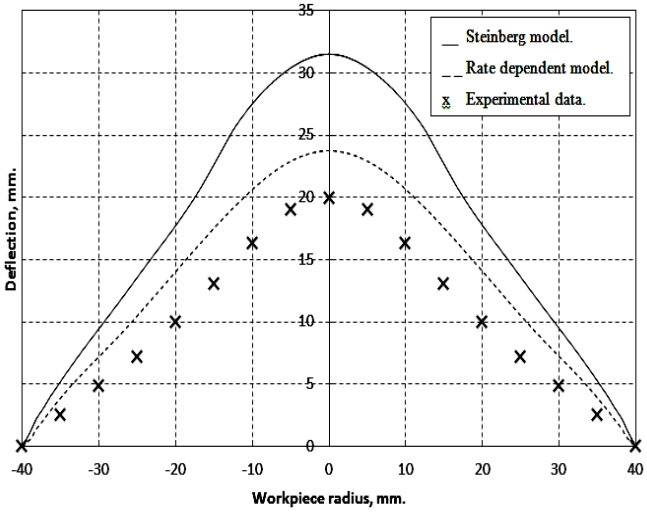

Fig. 9. Final profile of deformed workpiece with using various hardening models.

The relative errors between simulation results and experimental work are calculated over the whole deformed workpiece and presented in Fig. (10). The maximum relative error was about 90 % for Steinberg model while it was about 45 % rate dependent hardening model. It is obvious that the most accurate strain hardening model is rate dependent power law which has a relative error with average value over disk radius of 30 %. This result is logic since the strain rate in this process has very large values and can't be neglected.

The effective plastic strain distribution on the final deformed disk is shown in Fig. (11). It is clear that a maximum value of effective plastic strain of 0.45 was achieved at blank

centre for rate dependent strain hardening model. For the other strain hardening model; the maximum effective plastic strain value was achieved at blank edge which may be not true.

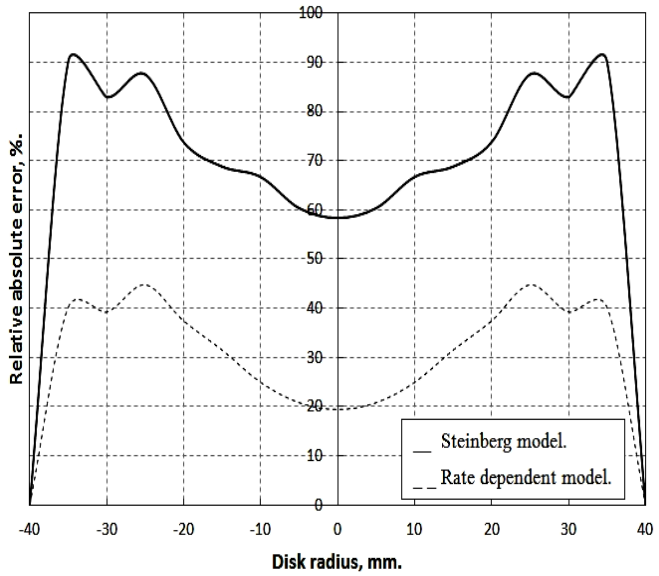

Fig. 10.Relative absolute error between FEM simulation and experimental data.

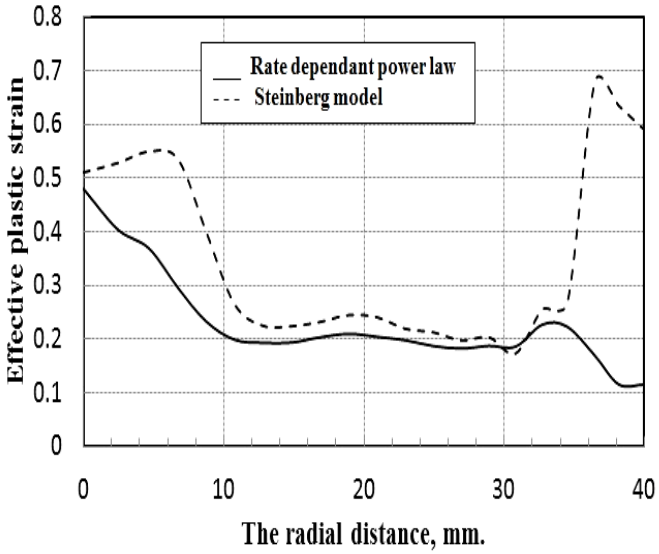

Fig. 11. Effective plastic strain distribution.

Effective plastic strain rate for elements at blank centre and at radial distance of 20 mm are plotted against time as shown in Fig. (12) and (13). It can be noticed that the maximum strain rate over the whole blank attained at centre. The strain rate at blank centre has its maximum value near end of deformation on contrast with strain rate at radial distance 20 mm. This could be explained by the earlier movement of blank outer perimeter than inner perimeters.

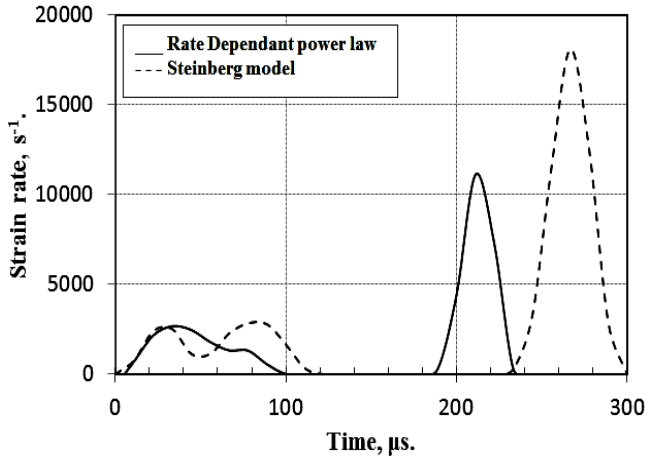

Fig. 12. Effective strain rate variation with time for element at blank centre.

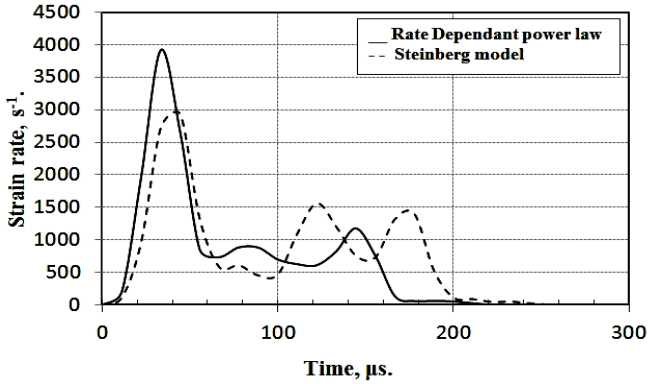

Fig. 13. Effective strain rate variation with time for element at 20 mm from centre.

4 CONCLUSIONS

In the current investigations a simple and accurate finite element model for the EM forming of sheet metals was introduced. Two different strain hardening material models were considered in simulation and the obtained results were compared with published experimental data. From the simulation results and comparison between them the following points can be concluded:

1- The introduced simulation model gives simulation results in good agreement with experimental data when used with rate dependent power law hardening model. This is logic since high strain rates were achieved in this process and thus strain rate effects can't be neglected.

2- The final deformed blank profiles didn't have any change in shape for any used strain hardening model but the changes are only in dimensions of the final deformed blank. This means that the final profile depends mainly on the pressure spatial and temporal distribution.

3- For rate dependent power law model; maximum values of strains and strain rates are achieved at blank centre. This means that failure is possible to occur at centre of the blank.

REFERENCES

[1] Seth, M., Vohnout V. J., Daehn G. S., "Formability Of Steel Sheet In High Velocity Impact", J. mater. Process. Tech., 168, pp. 390-400, (2005).

[2] Padmanabhan, M., "Wrinkling And Springback In Electromagnetic Sheet Metal Forming And Electromagnetic Ring Compression", Master thesis, The Ohio State University, (1997).

[3] Takatsu, N., Kato, M., Sato, K., Tobe, T., "High Speed Forming Of Metal Sheets By Electromagnetic Force", J.S.M.E., 31(1), p. 142, (1988).

[4] Fenton, G. K., Daehn, G.S., "Modeling Of Electromagnetically Formed Sheet Metal", J. mater. Process. Tech., 75, pp. 6-16, (1998).

[5] Kondo, K., Suzuki, H. , "Research On The Accuracy Of Sheared Products By Different Working Principles In Precision Shearing", J. mater. Process. Tech., 56, pp. 70-77, (1996).

[6] El-Azab, A., Garnich, M., Kapoor, A., "Modeling Of The Electromagnetic Forming Of Sheet Metals: State-Of-The-Art And Future Needs", J Mater. Process. Tech., 142, pp. 744-754, (2003).

[7] Correia, J. P. M., Siddiqui, M.A., Ahzi, S., Belouettar, S., Davies, R., " A Simple Model To Simulate Electromagnetic Sheet Free Bulging Process.", Int. J. Mech. Sci., 50, pp. 1466-1475, (2008).

[8] Hashimoto, Y., Hideki, H., Miki, S., Hideaki, N. , "Local Deformation And Buckling Of A Cylindrical Al Tube Under Magnetic Impulsive Pressure", J Mater. Process. Tech., 85, pp. 209-212, (1999).

[9] Siddiqui, M. A., Correia, J. P. M., Ahzi, S., Belouettar, S., "A Numerical Model To Simulate Electromagnetic Sheet Metal Forming Process.", Int. J. Mater. Form., 1, pp. 1387-1390, (2008).

[10] Cui, X., Mo, J., Xiao, S., Du, E., Zhao, J., "Numerical Simulation Of Electromagnetic Sheet Bulging Based On FEM", Int. J. Adv. Manuf. Tech., pp. 1-8, (2011).

[11] Imbert, J. M., "Increased Formability and the Effects of the Tool/Sheet Interaction in Electromagnetic Forming of Aluminum Alloy Sheet", M.Sc., University of Waterloo, (2005).

[12] Oliveira, D. A., "Electromagnetic Forming of Aluminum Alloy Sheet: Experiment and Model.", M.Sc., University of Waterloo, (2002).

[13] Pérez, I., Aranguren, I, González, B, Eguia, I, "Electromagnetic Forming: A New Coupling Method", Int. J. Mater. Form., 2, pp. 637-640, (2009).

[14] Xu, W., Fang, H., Xu, W., "Analysis Of The Variation Regularity Of The Parameters Of The Discharge Circuit With The Distance Between Workpiece And Inductor For Electromagnetic Forming Processes", J. mater. Process. Tech., 203, pp. 216-220, (2008).

[15] Zhang, H., Murata, M., Suzuki, H., "Effects Of Various Working Conditions On Tube Bulging By Electromagnetic Forming", Journal of Materials Processing Technology, 48, pp. 113-121, (1995).

[16] Kleiner, M., Beerwald, C., Homberg, W., "Analysis of Process Parameters and Forming Mechanisms within the Electromagnetic Forming Process", Annals of the CIRP, 54, pp. 225-228, (2005).

[17] Yu, H. P., Li, C.F., Deng, J.H. , "Sequential Coupling Simulation For Electromagnetic Mechanical Tube Compression By Finite Element Analysis", J. Mater. Process. Tech., 209, pp. 707-713, (2009).